Error Modeling and Integrity Risk Analysis in SPP

Yuan Song, Qingsong Li, Yi Dong, Wanli Jian, Dingjie Wang, and Jie Wu(✉)

National University of Defense Technology, Changsha, China
songyuan97@qq.com, Wujie_nudt@sina.com

Abstract. With the popularity and development of GNSS, the concept of integrity is proposed in order to ensure the safety of navigation and positioning. In some related fields such as civil aviation and lifesaving, the requirements for the integrity are becoming stricter, making the Integrity Monitoring a hot issue to be solved urgently. However, the existing methods for this problem are theoretically imperfect and the error model used can't accurately describe the actual error distribution. In this article, we will first present a model for the observation error in single point positioning. Considering that the actual observation errors always have thick tails, a binormal error model has been raised. Next, based on the previous error model, we use the Robust Parameter Estimation (RPE) method based on predicted residual with single iteration to detect and exclude the fault observation values, and then calculate the positioning result. Finally, we derive a method for conservatively estimating the integrity risk in the position by segmenting and magnifying the test-passing domain. The experimental results show that compared with the single normal error model, our binormal error model can describe the actual error distribution better and is conservative in the tail. The RPE method based on predicted residual with single iteration has a good effect of detecting and excluding fault observations and has a small positioning error. When the theoretical risk is less than the risk threshold, the statistical integrity risk obtained from the data is also less than the threshold. In addition, in the case of a worse error distribution with larger fault probability and larger fault error variance, the integrity risk evaluation results are still credible, indicating our method has better robustness.

Keywords: SPP · Integrity Monitoring · Integrity risk analysis · Error modeling · FDE

1 Introduction

With the popularity and development of GNSS, the concept of Integrity is proposed to ensure the safety of navigation and positioning system which characterize the ability of a system to provide reliable positioning results and give alert in time when the positioning errors exceed the alarm limit. However, some inherent shortcomings of GNSS system limit its application in some fields like civil aviation and lifesaving because of their high demand in integrity. Therefore, it's very necessary to enhance a system's integrity in application in order to further improve its performance.

J. Sun et al. (Eds.): CSNC 2020, LNEE 651, pp. 651–662, 2020.
https://doi.org/10.1007/978-981-15-3711-0_58

The commonly used technique for the enhancement of GNSS integrity is monitoring which can give prompt alerts when the positioning error exceeds the alarm limit. The monitoring technology can mainly be separated into two categories, i.e. the internal method and external method. The external method is realized by setting ground monitoring station to monitor the failure in the whole satellite system and send the error correction factor with its integrity to users. In contrast, the internal method is based on satellite or user systems' internal redundant information. GNSS can monitor satellites' failures in it and send this information to users by navigation message but may react too slow to unpredictable failure, making it unable to satisfy the real-time requirement for some carriers. As a comparison, the Receiver Autonomous Integrity Monitoring (RAIM) method using the redundant information within receivers to perform integrity monitoring is better developed with wider application [1].

The RAIM is a method based on the consistency check of redundancy of measurements within receivers, which is first proposed by R.M. Kalafus in 1987 [2]. Traditional RAIM methods are mainly snapshot algorithms such as range comparison (RC) [3], parity vector method (PV) [4], lest-squares residuals (LSR) [5].

However, when using traditional RAIM methods to detect errors, the number of visible satellites is demanded. At least 5 satellites are required to detect a failure and 6 to exclude it. Apart from that, traditional RAIM mainly aims at failures caused by large measurement errors and can exclude only one failure at one time. At the same time, it provides integrity evaluation only in the horizontal direction, which limits its application in precision approach.

To overcome the aforementioned limitations of RAIM, ARAIM is proposed which constructs statistical test values based on multiple solution assumption and separation method. Compared with RAIM, ARAIM can be used under multiple failures and constellations, eliminating the ionosphere delay by dual frequency observation. At the same time, integrity risk can be appropriately allocated through RAIM.

However, these classical methods are still far from perfection. For example, zero-mean Gauss model are adopted by most of these methods, but the realistic measurement errors always have thick tails, which makes the model fails to cover large errors at the tail area which have small probability to appear. Besides, when calculating the positioning error protection limits, the definition of fault error is not clear enough, and the results may be too conservative, making the in theory incomplete. To solve the problems stated above, this paper proposed a new error model, with related parameter estimation and integrity analysis method, which can give the estimated value of integrity risk directly.

This paper is organized as follows. In Sect. 2, a binormal error model is first proposed for describing the observation error in pseudo-range Single Point Positioning (SPP). Then, we use RPE method based on predicted residual with single iteration to detect and exclude fault measurement using predicted residuals, and future the positioning solution is calculated. At last, a method for conservatively estimating integrity risk is given based on the segmentation and amplification of test-passing domain. In Sect. 3, three different fault environments are designed with given fault error parameters and risk threshold to verify the method proposed in this paper. Furthermore, a robustness test is set to verify whether the method is still credible when the true error is underestimated. At the same time, the Least Square (LS) Method is introduced for comparison. In Sect. 4, a conclusion is drawn to summarize the proposed method and the simulation results.

2 Research Method

2.1 Error Model

When we draw the statistical histogram of the measurement errors in single point positioning, we found that the errors don't completely satisfy the normal distribution, and in most cases have thick tails. In order to make the error model more conservative at the tail, a binormal distribution model is established. The overall error ε is described by the normal error ε_0, the fault error ε_f and the probability of fault P_f:

$$\varepsilon = \varepsilon_0 + k \bullet \varepsilon_f \tag{1}$$

Where

$$k = \begin{cases} 0 & (1 - P_f) \\ 1 & P_f \end{cases}, \quad \varepsilon_0 \sim N_0(0, \quad \sigma_{Mid}^2), \quad \varepsilon_f \sim N_f(0, \quad \sigma_{Tail}^2, \quad \varepsilon_T) \tag{2}$$

The normal error obeys a normal distribution with a mean of 0 and a variance of σ_{Mid}^2, and the fault error obeys a normal distribution with a mean of 0, a variance of σ_{Tail}^2, an error threshold of ε_T. The probability density function (PDF) of ε_0 and ε_f is shown in Fig. 1.

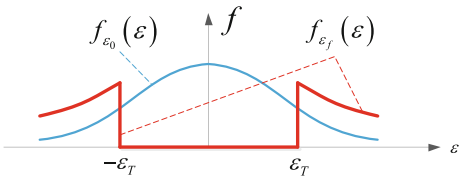

Fig. 1. PDF of normal error and fault error

The error model in Eq. (1) has four unknown parameters: σ_{Mid}, σ_{Tail}, P_f, ε_T, which can be obtained from statistical histogram. From these four parameters, the relevant variances can be calculated in Eq. (3).

$$\sigma_0^2 = \int_{-\infty}^{+\infty} \varepsilon^2 \bullet f_{\varepsilon_0}(\varepsilon) \bullet d\varepsilon, \quad \sigma_f^2 = \int_{-\infty}^{+\infty} \varepsilon^2 \bullet f_{\varepsilon_f}(\varepsilon) \bullet d\varepsilon, \quad \sigma^2 = \sigma_0^2 + P_f \bullet \sigma_f^2 \tag{3}$$

The distribution density function of ε can be calculated as follow:

$$f(\varepsilon) = (1 - P_f) \bullet f_{\varepsilon_0}(\varepsilon) + P_f \bullet f_{(0+f)}(\varepsilon) \tag{4}$$

And the calculation of $f_{(0+f)}(\varepsilon)$ is shown in Eq. (5).

$$f_{(0+f)}(\varepsilon) = \int_{-\infty}^{+\infty} f_{\varepsilon_0}(x) f_{\varepsilon_f}(\varepsilon - x) dx \tag{5}$$

2.2 RPE Method Based on Predicted Residual with Single Iteration

2.2.1 The Calculation of Predicted Residual

The observation equation of SPP is shown in Eq. (6) [6].

$$\mathbf{Y}_{n\times 1} = \mathbf{A}_{n\times 4}\mathbf{X}_{4\times 1} + \boldsymbol{\varepsilon}_{n\times 1} \tag{6}$$

Then the predicted residual T_i in each channel can be calculated as follows:

$$T_i = y_i - y_i^{'}, \quad y_i^{'} = \vec{\mathbf{a}}_\mathbf{i} \bullet \hat{\mathbf{x}} = \vec{\mathbf{a}}_\mathbf{i} \bullet \left(\mathbf{A}_\mathbf{i}^\mathbf{T}\mathbf{G}_\mathbf{i}\mathbf{A}_\mathbf{i}\right)^{-1}\mathbf{A}_\mathbf{i}^\mathbf{T}\mathbf{G}_i \bullet \vec{\mathbf{y}} \tag{7}$$

Where n is the number of satellites, y_i is the observation value, $y_i^{'}$ is the predicted observation, $\vec{\mathbf{a}}_\mathbf{i}$ is the direction cosine vector from the observation station to the corresponding satellite, $\mathbf{A_i}$ is the direction cosine matrix after removing $\vec{\mathbf{a}}_\mathbf{i}$, $\mathbf{G_i}$ is the observation weight matrix after removing y_i.

Assuming ε_i is the true measurement error, ε_i' is the predicted error. Then T_i and the variance variance of T_i can be calculated as follows:

$$T_i = \varepsilon_i - \varepsilon_i', \quad \sigma_{T,i}^2 = \sigma_i^2 + \sigma_i'^2, \quad \sigma_i'^2 = \vec{\mathbf{a}}_\mathbf{i} \cdot \left(\mathbf{A}_\mathbf{i}^\mathbf{T}\mathbf{G}_\mathbf{i}\mathbf{A}_\mathbf{i}\right)^{-1} \cdot \vec{\mathbf{a}}_\mathbf{i}^\mathbf{T} \tag{8}$$

In the equation, σ_i is the standard deviation of the observation error in channel i, and σ_i' is the standard deviation of the predicted error.

2.2.2 Parameter Estimation Method

First, we detect and exclude errors for each measurement channel. The steps are as follows:

(i) Assuming that T_i obeys a normal distribution, calculate the test threshold $T_{\alpha,i}$ for each channel using $P_{FA,0}$, the required false alarm rate.

$$T_{\alpha,i} = \Phi_{0,\sigma_{T,i}}\left(1 - P_{FA,0}\right) \tag{9}$$

(ii) Compare the value of T_i and $T_{\alpha,i}$. If $T_i \le T_{\alpha,i}$, then the observation of this channel is regarded as normal. If $T_i > T_{\alpha,i}$, then the observation of this channel is regarded as fault, and the serial number i should be recorded.

(iii) Compare the number of serial numbers recorded with $(n-4)$. If the number is less, the system can't provide a positioning solution, and an integrity alarm should be given. Otherwise, the fault observation channels should be excluded.

Next, calculate the positioning solution $\hat{\mathbf{X}}$ using LS method, regarding the remaining observations as normal.

$$\hat{\mathbf{X}} = \left(\mathbf{A}^{\mathbf{T}}\mathbf{G}\mathbf{A}\right)^{-1}\mathbf{A}^{\mathbf{T}}\mathbf{G} \bullet \mathbf{Y}, \quad \mathbf{G} = diag\left(\sigma_{0,1}^2, \quad \cdots, \quad \sigma_{0,m}^2\right) \tag{10}$$

And m is the number of remaining observations.

2.3 Integrity Risk Evaluation

After fault detection and exclusion, fault observation may still exist in the remaining observations, so giving the integrity analysis of the positioning solution is necessary. The main idea of the analysis method is to divide the measurement domain into two parts according to the setting threshold, and then carry out conservative estimations inside and outside the threshold. However, if the threshold is set directly using the real error threshold ε_T, the integrity risk estimation value will be too conservative. So the concept of expected threshold is proposed, which can be adjusted to make the conservative degree of risk estimation value more reasonable. The detailed methods will be given below.

2.3.1 Evaluation Methods

Define the following areas:

$$\begin{aligned} &S_{t,0} = \{\varepsilon_i || \varepsilon_i| \le \varepsilon_T\}, \quad S_{t,f} = \{\varepsilon_i || \varepsilon_i| > \varepsilon_T\}, \quad S_r = \left\{\left(\varepsilon_i, \varepsilon_i'\right) \middle| \left|\varepsilon_i - \varepsilon_i'\right| \le T_\alpha\right\} \\ &S_{exp,0} = \left\{\left(\varepsilon_i, \varepsilon_i'\right) || \varepsilon_i| \le \varepsilon_\xi\right\}, \quad S_{exp,f} = \left\{\left(\varepsilon_i, \varepsilon_i'\right) || \varepsilon_i| > \varepsilon_\xi\right\} \\ &S_{r,0} = \left\{\left(\varepsilon_i, \varepsilon_i'\right) \middle| \left|\varepsilon_i - \varepsilon_i'\right| \le T_\alpha \cap |\varepsilon_i| \le \varepsilon_\xi\right\}, \quad S_{r,f} = \left\{\left(\varepsilon_i, \varepsilon_i'\right) \middle| \left|\varepsilon_i - \varepsilon_i'\right| \le T_\alpha \cap |\varepsilon_i| > \varepsilon_\xi\right\} \end{aligned} \tag{11}$$

The positions of the above areas in the plane formed by ε_i and ε_i' are shown in Fig. 2, where ε_ξ is the expected error threshold, and $S_{exp,0}$ is the expected-passing domain.

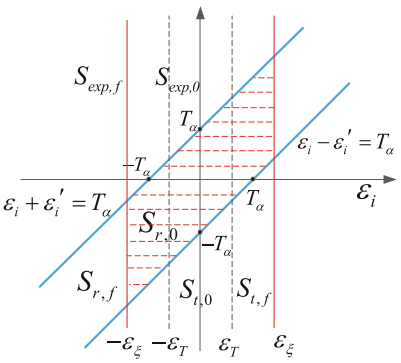

Fig. 2. Regional distribution in error plane

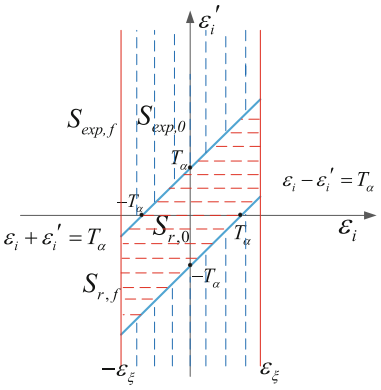

Fig. 3. Expansion of the error distribution in the expected domain

Accordingly, the following events are defined:

$$\begin{aligned} &A_{r,i} : \varepsilon_i \in S_{r,i}, \quad A_{r,0,i} : \varepsilon_i \in S_{r,0,i}, \quad A_{r,f,i} : \varepsilon_i \in S_{r,f,i} \\ &A_{e,0,i} : \varepsilon_i \in S_{e,0,i}, \quad A_{e,f,i} : \varepsilon_i \in S_{e,f,i}, \quad \bar{B} : |\triangle x| > AL \end{aligned} \tag{12}$$

Then the overall integrity risk can be expressed as follows:

$$P_{HMI} = P\left\{ (|\triangle x| > AL) \cap \left(\bigcap_{i=1}^{n} \varepsilon_i \in S_{r,i} \right) \right\} = P\left(\bar{B} \cdot \prod_{i=1}^{n} A_{r,i} \right) \tag{13}$$

After derivation, the following conclusions were established:

$$P_{HMI} \leq P\left(\bar{B} \cdot \prod_{i=1}^{n} A_{r,0,i} \right) + \sum_{i=1}^{n} P\left(A_{r,f,i}\right) = P_{HMI,1} + P_{HMI,2} \tag{14}$$

Therefore, the integrity risk can be divided into two parts according to the expected threshold ε_ξ.

Inside the expected domain, we expand the error space $S_{r,0,i}$ into $S_{e,0,i}$, as is shown in Fig. 3. Then the two-dimensional error integration can be simplified into one-dimensional error integration of ε_i inside ε_ξ, and the integrity risk $P_{HMI,1}$ can be calculated conservatively as follows:

$$\begin{aligned} P_{HMI,1} &= P\left(\bar{B} \cdot \prod_{i=1}^{n} A_{r,0,i} \right) \leq P\left(\bar{B} \cdot \prod_{i=1}^{n} A_{exp,0,i} \right) \\ &= P\left(\bar{B} \middle| \prod_{i=1}^{n} A_{exp,0,i} \right) \bullet P\left(\prod_{i=1}^{n} A_{exp,0,i} \right) \end{aligned} \tag{15}$$

Outside the expected passing domain, the calculation of integrity risk is transformed into the sum of the missed alarm rate of each channel (the area of the dotted line in Fig. 4, which requires two-dimensional integration of the joint distribution density function, and is computationally intensive.

To simplify the calculation, we transform the missed alarm rate into the products of the one-dimensional integral of ε_i' at ε_ξ (the area of the dotted line in Fig. 5) and the probability that the measurement error exceeds ε_ξ. Then we can calculate $P_{HMI,2}$ as follows:

$$\begin{aligned} P_{HMI,2} &= \sum_{i=1}^{n} P\left(A_{r,f,i}\right) \\ P\left(A_{r,f,i}\right) &= \iint_{S_{r,f,i}} f_{\varepsilon_i}(\varepsilon) f_{\varepsilon_i'}(\varepsilon) d\varepsilon \ \leq P\left(|\varepsilon_i| \geq \varepsilon_{\xi,i}\right) \cdot \int_{\varepsilon_{\xi,i} - T_{\xi,i}}^{\varepsilon_{\xi,i} + T_{\xi,i}} f_{\varepsilon_i'}(\varepsilon) d\varepsilon \end{aligned} \tag{16}$$

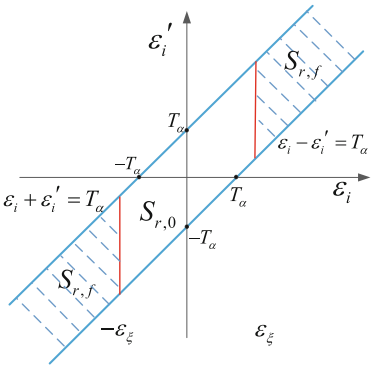

Fig. 4. The missed inspection area outside the expected domain

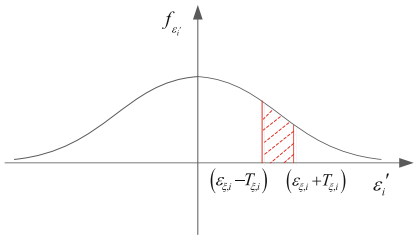

Fig. 5. PDF of the reported observation error

Assuming that there are zero, one, and multiple faults in the remaining measurement channels, and then calculate the integrity risk under each fault hypothesis. Here, we take the first fault hypothesis as an example to show the process of integrity risk analysis.

The probability of occurrence of the first fault hypothesis P_0 is the probability that all the remaining channels are normal:

$$P_0 = \left(1 - P_f\right)^{n-1} \tag{17}$$

Then the integrity risk of this fault hypothesis $P_{HMI,2,0}$ can be calculated:

$$\begin{aligned} P_{HMI,2,0} &= P\left(\varepsilon_i \geq \varepsilon_{\xi,i}\right) \cdot \left[\Phi_{0,\sigma'_{i,0}}\left(\varepsilon_{\xi,i} + T_{\xi,i}\right) - \Phi_{0,\sigma'_{i,0}}\left(\varepsilon_{\xi,i} - T_{\xi,i}\right)\right] \\ \sigma'^2_{i,0} &= \mathbf{A}_i \cdot \left(\mathbf{A}_i^T \mathbf{G}_{i,0} \mathbf{A}_i\right)^{-1} \cdot \mathbf{A}_i^T, \quad \mathbf{G}_{i,0} = diag\left(\sigma^2_{0,1}, \quad \cdots, \quad \sigma^2_{0,n-1}\right)^{-1} \end{aligned} \tag{18}$$

Using the same way, we can calculate the probability of the other two fault hypotheses P_1, P_2 and the corresponding integrity risks $P_{HMI,2,1}$, $P_{HMI,2,2}$. Then we can calculate $P_{HMI,2}$, the overall integrity risk outside the expected passing domain:

$$P_{HMI,2} = P_0 \cdot P_{HMI,2,0} + P_1 \cdot P_{HMI,2,1} + P_2 \cdot P_{HMI,2,2} \tag{19}$$

Finally, the overall integrity risk P_{HMI} is the sum of $P_{HMI,2}$ and $P_{HMI,1}$:

$$P_{HMI} = P_{HMI,1} + P_{HMI,2} \tag{20}$$

3 Simulation Experiment and Analysis

3.1 Simulation Results in Different Fault Environments

In order to verify the accuracy of the integrity analysis method above, we chose a set of single epoch pseudorange observation equations in a navigation experiment in Changsha on December 12, 2018 to carry out simulation experiments. The number of satellites is 9, corresponding to different elevation angles. Considering that the variance of the observation error is related to the elevation angle, we set the error model parameters as follows:

$$\sigma_{Mid} = \sqrt{\frac{\sigma_0^*}{sin\theta}}, \quad \sigma_{Tail} = k_f \bullet \sigma_{Mid}, \quad \varepsilon_T = 3 \bullet \sigma_{Mid} \tag{21}$$

In the equation, σ_0^* is the standard deviation of the zenith direction, and is set 1 m in the simulation. By setting the parameters and the probability of failure to different sizes, three fault environments are set, corresponding to different risk thresholds and alarm limits. The specific parameter settings are as follows (Table 1).

Table 1. Parameter settings in the three fault environments

	P_f	k_f	$P_{HMI,0}$	$P_{FA,0}$	$HAL(m)$	$VAL(m)$
Environment 1	0.01	20	5×10^{-3}	1×10^{-3}	30	40
Environment 2	0.005	15	5×10^{-4}	1×10^{-4}	20	30
Environment 3	0.001	10	5×10^{-5}	1×10^{-5}	15	20

Among them, $P_{HMI,0}$ is the threshold of integrity risk, $P_{FA,0}$ is the threshold of false alarm rate, HAL is the horizontal positioning error alarm limit, VAL is the vertical positioning error alarm limit.

By the time using RPE method based on predicted residual with single iteration and the integrity analysis method proposed in this paper, the Least Square (LS) method is introduced for comparison, in which the observation values are projected into the position domain to obtain a LS positioning solution, without detection and exclusion. The positioning error is regarded as a normal distribution, and the probability of exceeding the alarm limit is calculated, which is the integrity risk assessment value of the LS method.

Using the above two methods, the simulation is carried out in three different fault environments, and the statistical integrity risk is calculated, that is the statistical probability when calculated theoretical integrity risk is lower than the threshold but the actual positioning error exceeds the alarm limit. If the statistical integrity risk is less than the risk threshold, it means that the calculation of theoretical risk is credible.

The integrity risk thresholds in the three environments and the statistical integrity risk obtained by the two methods are shown in Table 2.

Table 2. Statistical integrity risk in the three fault environments

	$P_{HMI,0}$	RPE method	LS method
Environment 1	5×10^{-3}	1.3×10^{-3}	1.3×10^{-3}
Environment 2	5×10^{-4}	5×10^{-5}	2.6×10^{-3}
Environment 3	5×10^{-5}	6.0×10^{-6}	1.48×10^{-4}

The second row in Table 2 is the statistical integrity risk obtained by using proposed RPE and integrity analysis method, which is smaller than the threshold in the first row in all three environments, indicating the theoretical integrity calculated by this method is credible.

The third row in Table 3 is the statistical integrity risk obtained by using the LS method. It can be seen that except for the first fault environment, the risk threshold is greater than the threshold, indicating that the theoretical integrity calculated by this method is not credible.

Taking the second fault environment as an example, the statistical error randomly generated according to the set parameters and theoretical distribution curve of the first satellite is shown in Fig. 6. It can be seen that the simulation error is consistent with the theoretical distribution both in the middle and the tail, which is the basic guarantee for future detection and analysis.

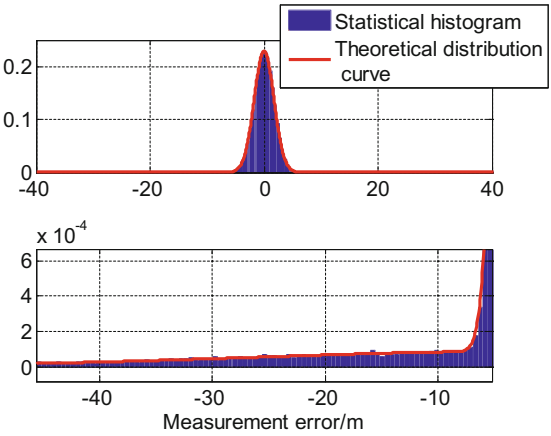

Fig. 6. Statistical histogram of measurement error and the theoretical distribution curve

The risk output graph and the positioning error output graph in the simulation process for the second fault environment are shown in Figs. 7 and 8.

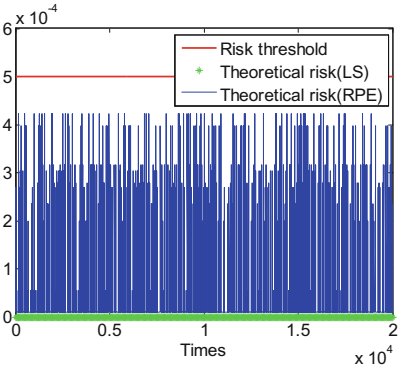

Fig. 7. Integrity risk diagram during simulation

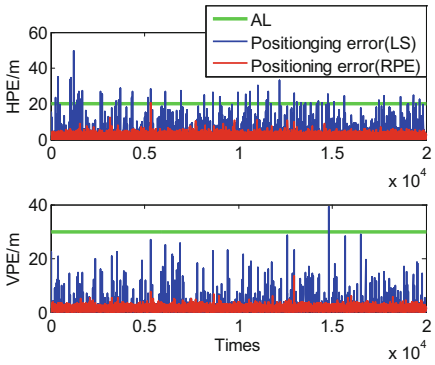

Fig. 8. Positioning error diagram during simulation

It can be seen from the figures that neither of the two methods gives an integrity waring during the simulation process, so the continuity risk meets the requirements. In the actual positioning results, only one of the positioning error (PE) obtained using the proposed RPE and integrity analysis method exceeded the given alarm limit, however, the positioning errors obtained using LS method exceeded the alarm limit multiple times.

In addition, it should be noted that the LS method used in this paper refers to the method of performing least square calculation directly using observations and estimating integrity risk without fault detection and exclusion. For the purpose of accelerating the verification of the integrity risk, the probability of fault and fault error parameters set in this paper are greater than the actual situation, so the positioning error obtained by suing the LS method is larger. By comparing the results of the two methods, it's clear that the proposed RPE and integrity analysis method has a good effect of excluding fault errors, and the integrity risk analysis are credible.

3.2 Robustness Test of Integrity Analysis Method

Since the error modelling is performed by fitting the actual measured error, it may not be able to accurately describe the real error distribution. Therefore, it is necessary to perform a robustness test on the proposed integrity analysis method. When generating measurement error, we set the real standard deviation and the fault occurrence probability higher than the estimated value, so that we can verify whether the calculated theoretical integrity risk is still credible when the true error is underestimated.

In the three fault environments, the given error parameters and the real parameters used in the actual simulation are shown in Table 3.

Table 3. Parameter settled and actually used in the three fault environments

	$P_f(settled)$	$P_f\,(real)$	$k_f\,(settled)$	$k_f\,(real)$
Environment 1	0.01	0.02	20	25
Environment 2	0.005	0.01	15	20
Environment 3	0.001	0.002	10	15

Table 4 shows the integrity risk thresholds and the statistical integrity risk for the two methods in the three environments.

Table 4. Statistical integrity risk in the three fault environments

	$P_{HMI,0}$	RPE method	LS method
Environment 1	5×10^{-3}	3.6×10^{-3}	1.05×10^{-2}
Environment 2	5×10^{-4}	4.0×10^{-4}	1.15×10^{-2}
Environment 3	5×10^{-5}	3×10^{-5}	3.31×10^{-3}

As cans be seen from Table 4, in the three fault environments, even if there is a certain deviation between the estimation error and the true error, the statistical integrity risk obtained by using proposed RPE and integrity analysis method in the second row is still smaller than the risk thresholds in the first row, indicating that this method has robustness. However, the LS method doesn't have such robustness. The statistical integrity risk in the third row is far beyond the risk threshold, showing the evaluation result not credible.

4 Summary

Aiming at the "thick tail" characteristic of actual observation error, this paper designs a double normal error model, which uses four parameters to describe the distribution characteristics of the error, making the error more conservative at the tail. Based on this error model, a Robust Parameter Estimation (RPE) method based on predicted residual with single iteration and the corresponding integrity analysis method is designed. The predicted residual of each channel is used as the test statistic to detect and elect fault observations using a certain strategy. Then the expected threshold is introduced among the observations that passed the test to split the overall integrity risk into two parts, performing conservative calculations for each part.

The simulation results show that for different fault environments, the RPE and integrity analysis method proposed in this paper have a good effect of excluding fault errors, and the calculated theoretical integrity risk is credible. At the same time, the method has a certain degree of robustness in the case of underestimation of the true measurement error. In addition, the comparison with the LS method is introduced to further verify the superiority of the proposed method.

References

1. Huang, Z.: Radio Navigation Theory and Systems. Beijing University of Aeronautics and Astronautics Press, Beijing (2007)
2. Chen, J.: GPS integrity augmentation. The PLA Information Engineering University (2001)
3. Lee, Y.: Analysis of range and position comparison methods as a means to provide GPS integrity in the user receiver. In: Proceedings of the 42 Annual Meeting (1986)
4. Sturza, M.A.: Navigation system integrity monitoring using redundant measurement. NAVIGATION J. Inst. Navig. **35**(2), 483–501 (1988)
5. Parkinson, B.W., Axelrad, P.: Autonomous GPS integrity monitoring using the pseudorange residual. NAVIGATION J. Inst. Navig. **35**(2), 255–274 (1988)
6. Blanch, J., et al.: An optimized multiple solution separation RAIM algorithm for vertical guidance. In: Proceedings of the ION GNSS 2007 (2007)